Combustion and Flame 156 (2009) 1871–1885

Contents lists available at ScienceDirect

Combustion and Flame

journal homepage: www.elsevier.com/locate/combustflame

Combustion modeling of mono-carbon fuels using the rate-controlled constrained-equilibrium method

Mohammad Janbozorgi [a], Sergio Ugarte [a], Hameed Metghalchi [a,*], James. C. Keck [b]

[a] Mechanical and Industrial Engineering Department, Northeastern University, Boston, MA 02115, USA
[b] Mechanical Engineering Department, Massachusetts Institute of Technology, Cambridge, MA 02139, USA

ARTICLE INFO

Article history:
Received 15 September 2008
Received in revised form 2 February 2009
Accepted 25 May 2009
Available online 5 August 2009

Keywords:
Rate-controlled constrained-equilibrium
Maximum entropy principle
Detailed modeling
Reduced kinetics
Methane
Methanol
Formaldehyde

ABSTRACT

The rate-controlled constrained-equilibrium (RCCE) method for simplifying the kinetics of complex reacting systems is reviewed. This method is based on the maximum entropy principle of thermodynamics and involves the assumption that the evolution of a system can be described using a relatively small set of slowly changing constraints imposed by the external and internal dynamics of the system. As a result, the number of differential and algebraic equations required to determine the constrained-equilibrium state of a system can be very much smaller than the number of species in the system. It follows that only reactions which change constraints are required to determine the dynamic evolution of the system and all other reactions are in equilibrium. The accuracy of the method depends on both the character and number of constraints employed and issues involved in the selection and transformation of the constraints are discussed. A method for determining the initial conditions for highly non-equilibrium systems is also presented.

The method is illustrated by applying it to the oxidation of methane (CH_4), methanol (CH_3OH), and formaldehyde (CH_2O) in a constant volume adiabatic chamber over a wide range of initial temperatures, pressures, and equivalence ratios. The RCCE calculations were carried out using 8–12 constraints and 133 reactions. Good agreement with "Detailed Kinetic Model" (DMK) calculations using 29 species and 133 reactions was obtained. The number of reactions in the RCCE calculations could be reduced to 20 for CH_4, 16 for CH_3OH, and 12 for CH_2O without changing the results significantly affecting the agreement. It may be noted that a DKM with 29 species requires a minimum of 29 reactions.

1. Introduction

The development of models for describing the dynamic evolution of chemically reacting systems is a fundamental objective of chemical kinetics. The conventional approach to this problem involves first specifying the state and species variables to be included in the model, compiling a "full set" of rate-equations for these variables, and integrating this set of equations to obtain the time-dependent behavior of the system. Such models are frequently referred to as "Detailed Kinetic Model"s (DKMs).

The problem is that the detailed kinetics of C/H/O/N molecules can easily involve hundreds of chemical species and isomers, and thousands of possible reactions even for system containing only C_1 molecules. Clearly, the computational effort required to treat such systems is extremely large. The difficulties are compounded when considering reacting turbulent flows, where the complexity of turbulence is added to that of the chemistry.

As a result a great deal of effort has been devoted to developing methods for reducing the size of DMKs. Among the most prominent are: Quasi Steady State Approximation (QSSA) [1], Partial Equilibrium Approximation [2], Intrinsic Low Dimensional Manifolds (ILDM) [3], Computational Singular Perturbation (CSP) [4], Adaptive Chemistry [5], Directed Relation Graph (DRG) [6], and the ICE-PIC method [7].

An alternative approach, originally proposed by Keck and Gillespie [8] and later developed and applied by Keck and co-workers [9–11], and others [12–15] is the rate-controlled constrained-equilibrium (RCCE) method. This method is based on the maximum entropy principle of thermodynamics and involves the fundamental assumption that slow reactions in a complex reacting system impose constraints on its composition which control the rate at which it relaxes to chemical-equilibrium, while the fast reactions equilibrate the system subject to the constraints imposed by the slow reactions. Consequently, the system relaxes to chemical-equilibrium through a sequence of constrained-equilibrium states at a rate controlled by the slowly changing constraints.

An advantage of the RCCE method is that it does not require a large DKM as a starting point. Instead, one starts with a short list

* Corresponding author. Fax: +1 617 373 2921.
E-mail address: Metghalchi@coe.neu.edu (H. Metghalchi).

0010-2180/$ - see front matter © 2009 The Combustion Institute. Published by Elsevier Inc. All rights reserved.
doi:10.1016/j.combustflame.2009.05.013

of constraints and rate-limiting reactions, to which more can be added to improve the accuracy to the desired level. If the only constraints are those imposed by slowly changing state variables, the RCCE method is equivalent to a local-chemical-equilibrium (LTE) calculation. If the number of constraints in an RCCE model is identical to the number of species in a DKM model, then the total number of equations, differential plus algebraic, to be solved will be identical and the results will be similar but not identical to those of the DKM model. The DKM will include only the specified species whereas the RCCE model will include implicitly all species which can be made from the elements in the system.

As with all thermodynamic systems, the number of constraints necessary to describe the dynamic state of the system within measurable accuracy can be very much smaller than the number of species in the system. Therefore, fewer equations are required to describe the evolution of the system. A further advantage is that only rates of the slow constraint-changing reactions are needed and these are the ones most likely to be known. Reactions which do not change any constraint are in equilibrium and need not be specified. It should be emphasized that the successful implementation of the RCCE method depends critically on the constraints employed and a knowledge of the rates of the constraint-changing reactions is required. When rates are uncertain or unknown, the Principle of Bayesian Inference suggests that the best choice is to assume that the corresponding reactions are in constrained-equilibrium (CE).

The primary objectives of this paper are to: (1) review the working equations required to implement the RCCE method for chemically reacting systems, (2) discuss the issues involved in the selection and transformation of the constraints, and (3) present a method for determining the initial conditions for highly non-equilibrium systems, for which concentrations of some species are zero. To illustrate the method, RCCE calculations of the oxidation of C_1 hydrocarbons in a constant volume adiabatic chamber have been made and compared with the results of a DKM.

2. Rate-controlled constrained-equilibrium (RCCE) method

A detailed description of the rate-controlled constrained-equilibrium (RCCE) method is given in Ref. [16]. A concise summary of the working equations for chemically reacting gas mixtures is given below.

It is assumed that energy exchange reactions are sufficiently fast to equilibrate the translational, rotational, vibrational, and electronic degrees of the system subject to constraints on the volume, V, and the total energy, E, of the system. Under these conditions, the energy can be written

$$E = \underline{E}^T(T)\underline{N} \tag{1}$$

where $\underline{E}^T(T)$ is the transpose of the species molar energy vector, T the temperature and $\underline{N}$ is the vector of species mole numbers. It is further assumed that the perfect gas model applies and the species constraints, $\underline{C}$, can be expressed as a linear combination of the species mole numbers in the form

$$\underline{C} = \underline{\underline{A}}\,\underline{N} \tag{2}$$

where $\underline{\underline{A}}$ is the $n_c \times n_{sp}$ constraint matrix, n_c the number of constraints, n_{sp} the number of species and $\underline{C}$ and $\underline{N}$ are column vectors of length n_c and n_{sp}. Maximizing the entropy, $S(E, V, \underline{C})$, subject to the constraints (2) using the method of undetermined Lagrange multipliers, [16], we obtain the constrained-equilibrium composition of the system

$$\underline{N}^c = (M/p)\exp(-\underline{\mu}^\circ - \underline{\mu}^c) \tag{3}$$

where M is the total mole number, $p = MRT/V$ the pressure, and $\underline{\mu}^c = (\underline{h}^0 - T\underline{s}^0)$ is the dimensionless standard Gibbs free energy for n_{sp} species, and

$$\underline{\mu}^c = -\underline{\underline{A}}^T\underline{\gamma} \tag{4}$$

is the dimensionless constrained-equilibrium Gibbs free energy of the species. In Eq. (4), $\underline{\underline{A}}^T$ is the transpose of the constraint matrix, and $\underline{\gamma}$ is the vector of dimensionless constraint potentials (Lagrange multipliers) conjugate to the constraint vector, $\underline{C}$.

Given the values of the constraints, $\underline{C}$, and energy, E, of the system, substitution of Eq. (3) into Eqs. (1) and (2) gives a set of $n_c + 1$ transcendental equations which can be solved for the temperature, $T(E, V, \underline{C}, \underline{\mu}^\circ)$, and the constraint potentials, $\underline{\gamma}(E, V, \underline{C}, \underline{\mu}^\circ)$, using generalized equilibrium codes such as GNASA [17] or GSTANJAN [17]. Finally substituting Eq. (4) into Eq. (3) gives the constrained-equilibrium composition of the system, $\underline{N}^c(E, V, \underline{C}, \underline{\gamma})$.

2.1. Rate-equations for the constraints

It is assumed that changes in the chemical composition of the system are the results of chemical reactions of the type

$$\underline{\underline{\nu}}^-\underline{X} \leftrightarrow \underline{\underline{\nu}}^+\underline{X} \tag{5}$$

where $\underline{X}$ is the species vector $\underline{\underline{\nu}}^-$ and $\underline{\underline{\nu}}^+$ are $n_r \times n_{sp}$ matrices of stoichiometric coefficients of reactants and products, respectively, and n_r is the number of reactions. The corresponding rate-equations for the species can be written

$$\dot{\underline{N}} = V\underline{\underline{\nu}}\,\underline{r} \tag{6}$$

where $\underline{\underline{\nu}} = \underline{\underline{\nu}}^+ - \underline{\underline{\nu}}^-$, $\underline{r} = \underline{r}^+ - \underline{r}^-$, and $\underline{r}^+$ and $\underline{r}^-$ are the forward and reverse reaction rate column vectors of length n_r.

Differentiating Eqs. (1) and (2) with respect to time and using Eq. (6), we obtain equations for the energy

$$\dot{E} = \dot{T}\,\underline{C}_v^T\underline{N} + \underline{E}^T\dot{\underline{N}} \tag{7}$$

and constraints

$$\dot{\underline{C}} = \underline{\underline{A}}\,\underline{N} = V\underline{\underline{B}}\,\underline{r} \tag{8}$$

where

$$\underline{\underline{B}} = \underline{\underline{A}}\,\underline{\underline{\nu}} \tag{9}$$

is an $n_c \times n_r$ matrix giving the change of constraints due to the n_r elementary chemical reactions among species and $\underline{C}_v \equiv \partial\underline{E}/\partial T$ is the molar specific heat vector at constant volume. It follows from Eq. (9) that a reaction k for which all B_{ik} are zero will be in constrained-equilibrium and that a constraint i for which all B_{ik} are zero will be conserved. The latter is assumed to be the case for the elements.

Given equations for the state variables, $V(t)$ and $E(t)$, and initial values for the species, $\underline{N}(0)$, Eqs. (7) and (8) can be integrated in stepwise fashion to obtain the temperature, $T(t)$ and species constraints, $\underline{C}(t)$. At each time step, a generalized equilibrium code, such as GNASA or GSTANJAN previously cited, must be used to determine the temperature, $T(E, V, \underline{C}, \mu^\circ)$, and constrained-equilibrium composition, $\underline{N}^c(E, V, \underline{C}, \mu^\circ)$. These, in turn, can be used to evaluate the reaction rates $\underline{r}(T, V, \mu^\circ, \nu, \underline{N}^c)$ required for the next step. Note that only the rates of reactions which change constraints, i.e. those for which $B_{ik} \neq 0$, are required for RCCE calculations. All other reactions are in constrained-equilibrium and need not be specified.

2.2. Rate equations for the constraint potentials

Although direct integration of the rate-equations for the constraints is relative straight forward and simple to implement, it

has proved to be relatively inefficient and time consuming due to the slowness of the constrained-equilibrium codes currently available [17]. An alternative method, first proposed by Keck [16] and implemented in later works [18–19] with colleagues, is the direct integration of the rate-equations for the constraint potentials. This method has also recently been investigated by Tang and Pope [13] and Jones and Rigopoulos [14].

Differentiating Eq. (3) with respect to time and substituting the result into Eqs. (7) and (8) yields the $n_c + 1$ implicit equations for the energy,

$$\underline{\underline{D}}_{\Gamma}\dot{\underline{\gamma}} - D_V\frac{\dot{V}}{V} - D_T\frac{\dot{T}}{T} + \dot{E} = 0 \tag{10}$$

where

$$D_{\Gamma i} = \sum_j a_{ij}E_jN_j^c \tag{10a}$$

$$D_V = \sum_j E_jN_j^c \tag{10b}$$

$$D_T = \sum_j (C_{vj}T + E_j^2/RT)N_j^c \tag{10c}$$

and the constraint potentials,

$$\underline{\underline{C}}_{\Gamma}\dot{\underline{\gamma}} - \underline{C}_V\frac{\dot{V}}{V} - \underline{C}_T\frac{\dot{T}}{T} + \underline{\underline{Br}} = 0 \tag{11}$$

where

$$C_{\Gamma ik} = \sum_j a_{ij}a_{kj}N_j^c \tag{11a}$$

$$C_{Vi} = \sum_j a_{ij}N_j^c \tag{11b}$$

$$C_{Ti} = \sum_j a_{ij}E_jN_j^c/RT \tag{11c}$$

In this case, given equations for the state variables, $V(t)$ and $E(t)$, and the initial temperature, $T(0)$, and constraint potentials, $\underline{\gamma}(0)$, Eqs. (10) and (11) can be integrated using implicit ODE integration routines such as DASSL [20] to obtain the temperature, $T(t)$, and constraint potentials, $\underline{\gamma}(t)$. The constrained-equilibrium composition, $\underline{N}^c(E, V, t)$, of the system can then be determined using Eq. (3). The number of unknowns is reduced from the $n_{sp} + 1$ in a DKM calculation to $n_c + 1$ in the RCCE calculation. As previously noted, only the rate constants for those reactions which change constraints, i.e. $B_{ik} \neq 0$, are needed. Note that, once the constraint potentials have been determined, the constrained-equilibrium concentration of any species for which the standard Gibbs free energy is known can be calculated whether or not it is explicitly included in the species list. It also follows that all species are implicitly included in the RCCE rate-equations.

3. Selection of constraints

The careful selection of constraints is the key to the success of the RCCE method. Among the general requirements for the constraints are that they must (a) be linearly independent combinations of the species mole numbers, (b) hold the system in the specified initial state, (c) prevent global reactions in which reactants or intermediates go directly to products, and (d) determine the energy and entropy of the system within experimental accuracy. In addition, they should reflect whatever information is available about rate-limiting reactions which control the evolution of the system on the time scale of interest.

In the present work, the focus is on applications of the RCCE method to chemically reacting gas phase mixtures. In the temperature and pressure range of interest, the rates of nuclear and ionization reactions are negligible compared to those for chemical reactions and the fixed constraints are the *neutral elements* of hydrogen, carbon, oxygen, nitrogen, ... , designated by EH, EC, EO, EN, ...

Under these conditions, the slowest reactions controlling the chemical composition are three-body dissociation/recombination reactions and reactions which make and break valence bonds. Such reactions are slow in the endothermic direction because of the high activation energies required, and in the exothermic direction because of small three-body collision rates and small radical concentrations. They impose slowly varying time-dependent constraints on the number of *moles*, M, of gas and the *free valence*, FV, of the system, respectively. A finite value of FV is a necessary condition for chain branching chemical reactions to proceed.

A third important time-dependent constraint, imposed by slow OO bond-breaking reactions, is the *free oxygen*, FO, defined as any oxygen atom not directly bound to another oxygen atom. An increase in FO is a necessary condition for the formation of the major reaction products of hydrocarbon oxidation, H_2O, CO_2 and CO.

Two additional time-dependent constraints which slightly improve the agreement between RCCE and DKM calculations under some conditions are: OHO≡OH + O and DCO≡HCO + CO. The OHO constraint is a consequence of the relatively slow constraint-changing reaction RH + OH ↔ H_2O + R coupled with the fast reaction RH + O = OH + R which equilibrates OH and O. The DCO constraint is a consequence of the slow spin-forbidden reaction CO + HO_2 ↔ CO_2 + OH coupled with the fast reaction HCO + O_2 = CO + HO_2 which equilibrates HCO and CO.

For systems involving the elements C, H, and O the eight constraints EH, EO, EC, M, FV, FO, OHO, and DCO are independent of the initial reactants and may, therefore, be considered "universal" constraints. Along with the equilibrium reactions,

$$H_2 + O = OH + H \tag{CE1}$$

$$H_2 + HOO = H_2O_2 + H \tag{CE2}$$

$$HCO + O_2 = CO + HO_2 \tag{CE3}$$

they are sufficient to determine the constrained-equilibrium mole fractions of the 11 major hydrocarbon combustion products H, O, OH, HO_2, H_2, O_2, H_2O, H_2O_2, HCO, CO and CO_2 under both high and low temperature conditions.

In the present investigation of C_1 hydrocarbon oxidation, four additional fuel-dependent constraints have been used. The first is a constraint on the *fuel*, FU, imposed by slow hydrogen – abstraction reactions of the type FU + O_2 ↔ FR + HO_2 and even slower dissociation/recombination of the type AB + M ↔ A + B + M. This constraint is necessary to hold the system in its initial state. The second is a constraint on *fuel radicals*, FR, which is necessary to prevent the equilibration of forbidden exothermic global reactions such as $CH_3 + 2O_2 + 2H_2O = CO_2 + 2H_2O_2 + H_2 + H$ which would otherwise convert fuel radicals directly to major products. The third is a constraint on *alkylperoxides*, APO≡CH_3OOH + CH_3OO + CH_2OOH, imposed by slow reactions which convert APO to hydroperoxides coupled with fast reactions which equilibrate the species comprising APO, and the fourth is a constraint on *alcohol plus formaldehyde*, ALCD≡CH_3OH + CH_3O + CH_2OH + CH_2O imposed by relatively slow reactions which generate/remove ALCD coupled with fast reactions which equilibrate the species comprising ALCD.

3.1. Transformation of constraints

The integration of Eqs. (10) and (11) for the constraint potentials requires inversion of the $\underline{\underline{C}}_{\Gamma}$ matrix. The performance of the implicit integrators, such as DASSL, are quite sensitive to the structure of this matrix. In general, the codes work best when the large elements of the matrix lie on or close to the main diagonal. This is not usually the case for the initial set of constraints chosen and a

variety of error messages such as "singular matrix" or "failure to converge" may be encountered. The problem can almost always be solved by a transformation of the square sub-matrix relating the constraints and the major species to a diagonalized form. The physical meaning of the transformed matrix may not be clear in all cases but if it improves the speed and reliability of the integrator, the desired objective will have been achieved. In this connection, it is important to note that any linear combination of the original linearly independent constraints for which the integrator works should give the same final result. This can be a useful check on the numerical results.

A general transformation of the constraint matrix can be made as follows. Assume $\underline{\underline{G}}$ is a non-singular square transformation matrix of order n_c. Multiplying Eq. (2) through by this matrix yields

$$\underline{\tilde{C}} = \underline{\underline{G}}\,\underline{C} = \underline{\underline{\tilde{A}}}\,\underline{N} \tag{12}$$

where

$$\underline{\underline{\tilde{A}}} = \underline{\underline{G}}\,\underline{\underline{A}} \tag{13}$$

is the transformed $n_c \times n_{sp}$ constraint matrix that relates the transformed constraint vector, $\underline{\tilde{C}}$, to the species vector, $\underline{N}$. The corresponding transformation for the reaction matrix is

$$\underline{\underline{\tilde{B}}} = \underline{\underline{G}}\,\underline{\underline{B}} \tag{14}$$

The transformation equations for the constraint potentials can be obtained by noting that the Gibbs free energy, $\underline{\mu}^c$, is invariant under the transformation. Eq. (4) then gives

$$-\underline{\mu}^c = \underline{\underline{A}}^T\underline{\gamma} = \underline{\underline{\tilde{A}}}^T\underline{\tilde{\gamma}} = (\underline{\underline{G}}\,\underline{\underline{A}})^T\underline{\tilde{\gamma}} = \underline{\underline{A}}^T\underline{\underline{G}}^T\underline{\tilde{\gamma}} \tag{15}$$

Multiplying Eq. (15) by $\underline{\underline{A}}$ we obtain

$$-\underline{\underline{A}}\,\underline{\mu}^c = \underline{\underline{S}}\,\underline{\gamma} = \underline{\underline{S}}\,\underline{\underline{G}}^T\underline{\tilde{\gamma}} \tag{16}$$

where

$$\underline{\underline{S}} = \underline{\underline{A}}\,\underline{\underline{A}}^T \tag{17}$$

is a symmetric matrix of order n_c. Assuming that $\underline{\underline{S}}$ is non-singular, it follows from Eq. (16) that2

$$\underline{\gamma} = \underline{\underline{G}}^T\underline{\tilde{\gamma}} \tag{18a}$$

and, since $\underline{\underline{G}}$ is non-singular,

$$\underline{\tilde{\gamma}} = (\underline{\underline{G}}^T)^{-1}\underline{\gamma} \tag{18b}$$

4. Determination of initial conditions

For systems initially in a constrained-equilibrium state, the initial values of the constraint potentials are finite. However, for a system initially in a non-equilibrium state, where the concentrations of one or more species is zero, it can be seen from Eqs. (3) and (4) that one or more constraint potentials must be infinite. This condition is encountered in ignition-delay-time calculations, where the system is initially far from equilibrium and the initial concentrations of all species except the reactants are assumed to be zero.

One method of dealing with this problem is to assign small partial pressures to as many major product species as required to give finite values for the constraint potentials. Ideally the choice should be made in such a way that the partial pressures of all other product species will be smaller than the assigned partial pressures. A reasonable initial choice for a major species corresponding to a constraint is the species with the minimum standard Gibbs free energy in the group of species included in the constraint.

To implement this method, Eq. (2) is decomposed in the form

$$\underline{C} = \underline{\underline{A}}\,\underline{N} = \begin{bmatrix}\underline{\underline{A}}_{11} & \underline{\underline{A}}_{12}\end{bmatrix}\begin{bmatrix}\underline{N}_1\\ \underline{N}_2\end{bmatrix} \tag{19}$$

where $\underline{\underline{A}}_{11}$ is an $n_c \times n_c$ non-singular, square matrix giving the contribution of the major species vector, $\underline{N}_1$, to the constraint vector, $\underline{C}$, and $\underline{\underline{A}}_{12}$ is an $n_c \times (n_s - n_c)$ matrix, giving the contribution of $\underline{N}_2$ to $\underline{C}$. The corresponding decomposition of Eq. (4) is

$$\underline{\mu} = \begin{bmatrix}\underline{\mu}_1\\ \underline{\mu}_2\end{bmatrix} = -\underline{A}^T\underline{\gamma} = -\begin{bmatrix}\underline{\underline{A}}_{11}^T\\ \underline{\underline{A}}_{12}^T\end{bmatrix}\underline{\gamma} \tag{20}$$

Initial values for the constraint potentials can now be obtained by assuming $\underline{\mu}_1(0) \gg \underline{\mu}_2(0)$. This gives

$$\underline{\gamma}(0) = -(\underline{\underline{A}}_{11}^T)^{-1}\underline{\mu}_1(0) = -(\underline{\underline{A}}_{11}^T)^{-1}(\ln\underline{p}_1(0) + \underline{\mu}^\circ) \tag{21}$$

Having determined the initial values of the constraint potential vector, one can now check the assumption that the initial partial pressures of the minor species are small using the relation

$$\ln\underline{p}_2(0) = -\underline{\underline{A}}_{12}^T\underline{\gamma}(0) - \underline{\mu}_2^\circ \tag{22}$$

If they are not, an alternative choice for the major species will usually solve the problem.

In initial RCCE calculations using constraints based on kinetic considerations, problems involving the convergence of the implicit integrators used were frequently encountered. These were caused primarily by the fact the $\underline{\underline{C}}_{\Gamma}$ matrix in Eq. (11) contained large off diagonal elements. These problems were solved by a transformation which diagonalized the $\underline{\underline{A}}_{11}$ matrix. Using the transformation matrix $\underline{\underline{G}} = \underline{\underline{A}}_{11}^{-1}$ we obtain from Eq. (12)

$$\underline{\tilde{C}} = \underline{\underline{A}}_{11}^{-1}\underline{C} = \underline{\underline{A}}_{11}^{-1}\begin{bmatrix}\underline{\underline{A}}_{11} & \underline{\underline{A}}_{12}\end{bmatrix}\begin{bmatrix}\underline{N}_1\\ \underline{N}_2\end{bmatrix} = \begin{bmatrix}\underline{\underline{I}}_{11} & \underline{\underline{A}}_{11}^{-1}\underline{\underline{A}}_{12}\end{bmatrix}\begin{bmatrix}\underline{N}_1\\ \underline{N}_2\end{bmatrix} = \underline{\underline{\tilde{A}}}\,\underline{N} \tag{23}$$

and it follows from Eq. (15) that

$$\underline{\mu}_1(0) = \ln\underline{p}_1(0) + \underline{\mu}^\circ = -\underline{\underline{I}}_{11}\underline{\tilde{\gamma}}(0) = -\underline{\tilde{\gamma}}(0) \tag{24}$$

It can be seen from this equation, that in the diagonalized representation, the initial constraint potentials are simply the initial Gibbs free energies of the major species chosen as surrogates. The transformed reaction rate matrix is

$$\underline{\underline{\tilde{B}}} = \underline{\underline{A}}_{11}^{-1}\underline{\underline{B}} \tag{25}$$

5. RCCE calculations for C_1 hydrocarbon oxidation

To illustrate the RCCE method, we consider the homogeneous stoichiometric oxidation of three mono-carbon fuels, namely methane (CH_4), methanol (CH_3OH) and formaldehyde (CH_2O) with

Table 1
Definition of the constraints used in the present work.

	Constraint	Definition of the constraint
1	EC	Elemental carbon
2	EO	Elemental oxygen
3	EH	Elemental hydrogen
4	M	Total number of moles
5	FV	Moles of free valance (any unpaired valence electron)
6	FO	Moles of free oxygen (any oxygen not directly attached to another oxygen)
7	OHO	Moles of water radicals (O + OH)
8	DCO	Moles of HCO + CO
9	FU	Moles of fuel molecules
10	FR	Moles of fuel radicals
11	APO	Moles of alkylperoxides ($CH_3OO + CH_3OOH + CH_2OOH$)
12	ALCD	Moles of alcohols + aldehydes ($CH_3O + CH_3OH + CH_2OH + CH_2O$)

Table 2a
Constraint matrix $\underline{\underline{A}}$ for the C_1 system with 12 constraints and 29 species.

	1 CO_2	2 O_2	3 H_2	4 H_2O_2	5 HO_2	6 H_2O	7 HO	8 CO	9 CH_4	10 CH_3	11 CH_3OOH	12 H_2CO	13 H	14 CH_3O	15 HCO	16 CH	17 CH_2	18 C	19 O	20 CH_2OH	21 CH_3OH	22 HOCO	23 HOCHO	24 OCHO	25 CH_3OO	26 CH_2OOH	27 HOOCHO	28 HOOCO	29 OOCHO
EC	1	0	0	0	0	0	0	1	1	1	1	1	0	1	1	1	1	1	0	1	1	1	1	1	1	1	1	1	1
EO	2	2	0	2	2	1	1	1	0	0	2	1	0	1	1	0	0	0	1	1	1	2	2	2	2	2	3	3	3
EH	0	0	2	2	1	2	1	0	4	3	4	2	1	3	1	1	2	0	0	3	4	1	2	1	3	3	2	1	1
M	1	1	1	1	1	1	1	1	1	1	1	1	1	1	1	1	1	1	1	1	1	1	1	1	1	1	1	1	1
FV	0	0	0	0	1	0	1	0	0	1	0	0	1	1	1	3	2	4	2	1	0	1	0	1	1	1	0	1	1
FO	2	0	0	0	0	1	1	1	0	0	0	1	0	1	1	0	0	0	1	1	1	2	2	2	0	0	1	1	1
OHO	0	0	0	0	0	0	1	0	0	0	0	0	0	0	0	0	0	0	1	0	0	0	0	0	0	0	0	0	0
DCO	0	0	0	0	0	0	0	1	0	0	0	0	0	0	1	0	0	0	0	0	0	0	0	0	0	0	0	0	0
FU	0	0	0	0	0	0	0	0	1	0	0	0	0	0	0	0	0	0	0	0	0	0	0	0	0	0	0	0	0
FR	0	0	0	0	0	0	0	0	0	1	0	0	0	0	0	0	0	0	0	0	0	0	0	0	0	0	0	0	0
APO	0	0	0	0	0	0	0	0	0	0	1	0	0	0	0	0	0	0	0	0	0	0	0	0	1	1	0	0	0
ALCD	0	0	0	0	0	0	0	0	0	0	0	1	0	1	0	0	0	0	0	1	1	0	0	0	0	0	0	0	0

Table 2b
Diagonalized $\underline{\underline{A}}$ matrix for the C_1 system with 12 constraints and 29 species.

	1 CO_2	2 O_2	3 H_2	4 H_2O_2	5 HO_2	6 H_2O	7 HO	8 CO	9 CH_4	10 CH_3	11 CH_3OOH	12 H_2CO	13 H	14 CH_3O	15 HCO	16 CH	17 CH_2	18 C	19 O	20 CH_2OH	21 CH_3OH	22 HOCO	23 HOCHO	24 OCHO	25 CH_3OO	26 CH_2OOH	27 HOOCHO	28 HOOCO	29 OOCHO
CO_2	1	0	0	0	0	0	0	0	0	0	0	0	0	0	0	1	1	1	0	0	0	1	1	1	0	0	1	1	1
O_2	0	1	0	0	0	0	0	0	0	0	0	0	0	−1	−1	−2	−2	−2	0	−1	−1	−1	−1	−1	0	0	−1	−1	−1
H_2	0	0	1	0	0	0	0	0	0	0	0	0	1	0	0	2	2	2	0	0	0	0	0	0	0	0	0	0	0
H_2O_2	0	0	0	1	0	0	0	0	0	0	0	0	−1	0	0	−1	0	−2	−1	0	1	0	1	0	−1	−1	2	1	1
HO_2	0	0	0	0	1	0	0	0	0	0	0	0	1	1	1	3	2	4	1	1	0	1	0	1	1	1	0	1	1
H_2O	0	0	0	0	0	1	0	0	0	0	0	0	0	0	0	−2	−2	−2	0	0	0	0	0	0	0	0	−1	−1	−1
HO	0	0	0	0	0	0	1	0	0	0	0	0	0	0	0	0	0	0	1	0	0	0	0	0	0	0	0	0	0
CO	0	0	0	0	0	0	0	1	0	0	0	0	0	0	1	0	0	0	0	0	0	0	0	0	0	0	0	0	0
CH_4	0	0	0	0	0	0	0	0	1	0	0	0	0	0	0	0	0	0	0	0	0	0	0	0	0	0	0	0	0
CH_3	0	0	0	0	0	0	0	0	0	1	0	0	0	0	0	0	0	0	0	0	0	0	0	0	0	0	0	0	0
CH_3OOH	0	0	0	0	0	0	0	0	0	0	1	0	0	0	0	0	0	0	0	0	0	0	0	0	1	1	0	0	0
H_2CO	0	0	0	0	0	0	0	0	0	0	0	1	0	1	0	0	0	0	0	1	1	0	0	0	0	0	0	0	0

pure oxygen in a constant volume reactor over a wide range of initial temperatures (900–1500 K) and pressures (1–100 atm), and equivalence ratios (0.8–1.2). The 12 constraints used in the RCCE calculations are summarized in Table 1.

The DKM calculations with which the RCCE results are compared involve only C_1 chemistry and include 29 species and 133 reactions, without nitrogen chemistry. Twenty species and 100 reactions were taken from the widely known and used GRI-Mech3.0 [21] mechanism. This model does not include alkylperoxides and therefore is not expected to be valid under high pressure low temperature conditions. To obtain a model valid under these conditions an additional nine alkylperoxides and organic acids were included along with 33 reactions with rates taken from [22] or estimated by the authors.

Of the 133 reactions employed in the DKM calculations only 102 reactions change one or more of the constraints in Table 1 and are therefore of interest. The remaining 31 are in constrained-equilibrium and are not needed in RCCE calculations. In principle, only the fastest reaction in a group which changes a given constraint is required for a system to go from the specified initial state to the final chemical-equilibrium state determined by the elements. However, because the fastest reaction may change as the system evolves, it is usually necessary to include additional reactions to achieve the desired accuracy for the time evolution of the system.

In this work, excellent agreement between DKM calculations and RCCE calculations was obtained for all C_1 species using 12 constraints and 102 reactions and acceptable agreement was obtained using 12 constraints and 20 reactions for methane, 10 constraints and 16 reactions for methanol, and nine constraints and 12 reactions for formaldehyde.

5.1. Methane (CH_4) oxidation

The constraint matrix for CH_4 used in this work is shown in Table 2a and the corresponding diagonalized matrix used to set the initial conditions and carry out the numerical calculations is shown in Table 2b. 12 constraints and 29 species are included in the Tables. The corresponding RCCE reaction flow diagram is shown in Fig. 1. The constrained species are enclosed by dashed lines. Except for the initiation steps, this diagram also includes the sub-mechanisms involved in the oxidation of CH_3OH and CH_2O.

As can be seen, the oxidation process is initiated by the highly endothermic CH_4 constraint-changing H-abstraction reaction

$$CH_4 + O_2 \leftrightarrow CH_3 + HO_2 \quad \text{(RC1)}$$

This is followed by the two competing CH_3 constraint-changing reactions

$$CH_3 + O_2 + M \leftrightarrow CH_3OO + M \quad \text{(RC2)}$$
$$CH_3 + O_2 \leftrightarrow CH_3O + O \quad \text{(RC3)}$$

The first is most important at low temperatures and is followed by the constrained-equilibrium reactions

$$CH_3OO + H_2O_2 = CH_3OOH + HO_2 \quad \text{(CE1)}$$
$$CH_3OOH + HO_2 = CH_2OOH + H_2O_2 \quad \text{(CE2)}$$

which equilibrate the alkylperoxides in APO. The second is most important at high temperatures and is followed by the constrained-equilibrium reactions

$$H_2 + O = OH + H \quad \text{(CE3)}$$

which equilibrates the water radicals in OHO, and constrained-equilibrium reactions

$$CH_3O + H_2O_2 = CH_3OH + HO_2 \quad \text{(CE4)}$$
$$CH_3OH + HO_2 = CH_2OH + H_2O_2 \quad \text{(CE5)}$$
$$CH_3O + O_2 = CH_2O + HO_2 \quad \text{(CE6)}$$

which equilibrate the free oxygen species in ALCD. The CH_4 constraint-changing reaction

$$OH + CH_4 \leftrightarrow CH_3 + H_2O \quad \text{(RC4)}$$

converts OH in OHO to the product H_2O and regenerates CH_3.

The stable intermediate CH_2O in ALCD is oxidized by the constraint-changing H-abstraction reaction

$$CH_2O + O_2 \leftrightarrow CHO + HO_2 \quad \text{(RC5)}$$

and the constrained-equilibrium reaction and the fast equilibrium reaction

$$CHO + O_2 = CO + HO_2 \quad \text{(CE7)}$$

to form DCO. The CO in DCO is converted to the product CO_2 by the FO constraint-changing reaction

$$CO + HO_2 \leftrightarrow CO_2 + OH \quad \text{(RC6)}$$

Finally the eight major H/O species are determined by the four constraint-changing reactions

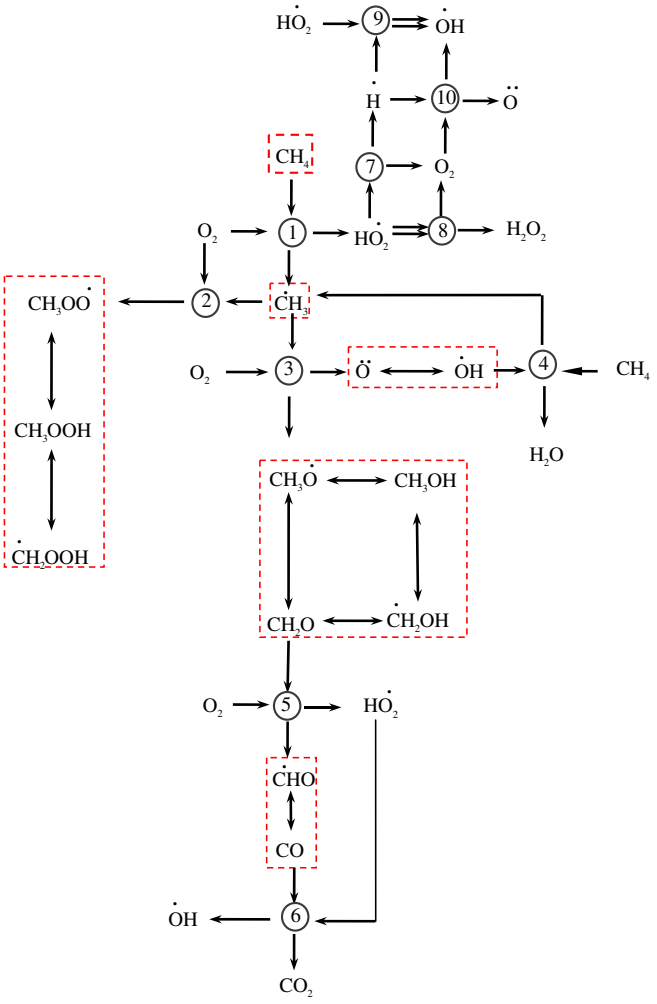

Fig. 1. RCCE reaction flow diagram for CH_4 oxidation.

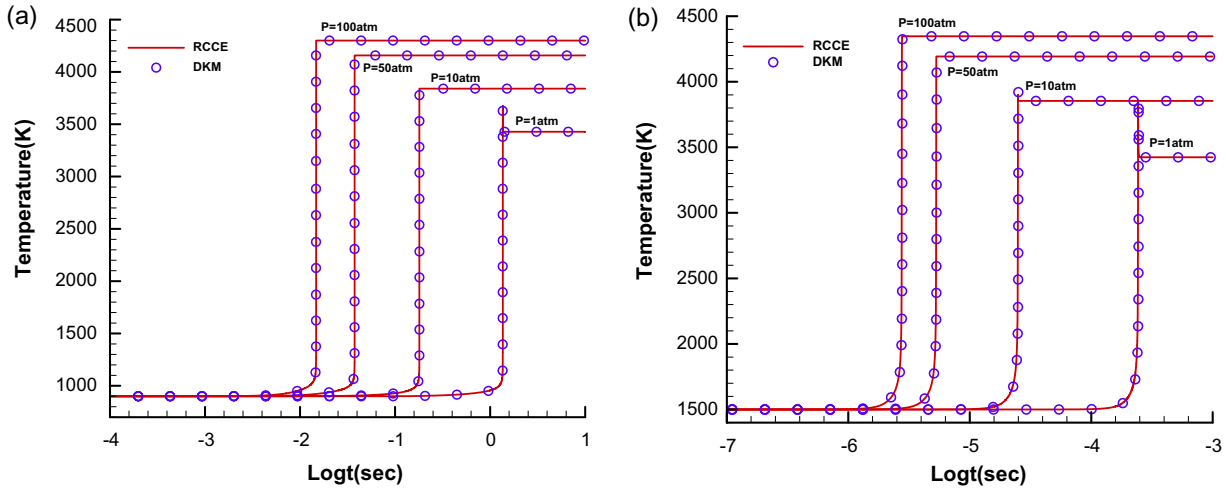

Fig. 2. Comparison of RCCE and DKM temperature vs. time profiles for a stoichiometric mixture of CH_4/O_2 at different initial pressures and initial temperatures of 900 K and 1500 K (time in s).

$$HO_2 \leftrightarrow H + O_2 \quad \text{(RC7)}$$

$$HO_2 + HO_2 \leftrightarrow H_2O_2 + O_2 \quad \text{(RC8)}$$

$$HO_2 + H \leftrightarrow OH + OH \quad \text{(RC9)}$$

$$H + O_2 \leftrightarrow OH + O \quad \text{(RC10)}$$

which change M, FV, FO, and OHO, respectively, plus the two constrained-equilibrium reactions

$$H_2 + O = OH + H \quad \text{(CE3)}$$

$$H_2 + HO_2 = H_2O_2 + H \quad \text{(CE8)}$$

and the elemental constraints EH and EO.

As the above reactions proceed, the radical population increases rapidly and all constraint-changing reactions included in the kinetic model become involved in determining the evolution of the system and its approach to final chemical-equilibrium. Of particular importance are reactions of the type

$$CH_4 + Q \leftrightarrow CH_3 + HQ \quad \text{(RC1.1)}$$

and

$$CH_2O + Q \leftrightarrow CHO + HQ \quad \text{(RC5.1)}$$

where Q can be any radical, e.g. HO_2, OH, H, O. Numbers in circles in Fig. 1 correspond to the rate-controlling reactions mentioned above, e.g. 1 corresponds to (RC1), 2 corresponds to (RC2) and so on.

5.1.1. CH_4 results for 133 reaction set

Time-dependent temperature profiles of stoichiometric mixtures of methane and oxygen at initial temperatures of 900 K and 1500 K and different initial pressures are shown in Fig. 2. All 12 constraints listed in Table 2a have been included. As previously noted, only 102 of the reactions in the full set of 133 reactions change constraints and are therefore required. The remaining 31 are in constrained-equilibrium and are not needed in RCCE calculations.

It can be seen that the agreement with DKM calculations is excellent over the entire range of pressure and temperature covered. Note that the temperature overshoot at low pressures due to slow three-body recombination and dissociation reactions is well reproduced by the constraint *M* on the total moles. Also, the same comparisons have been made for rich ($\phi = 1.2$) and lean

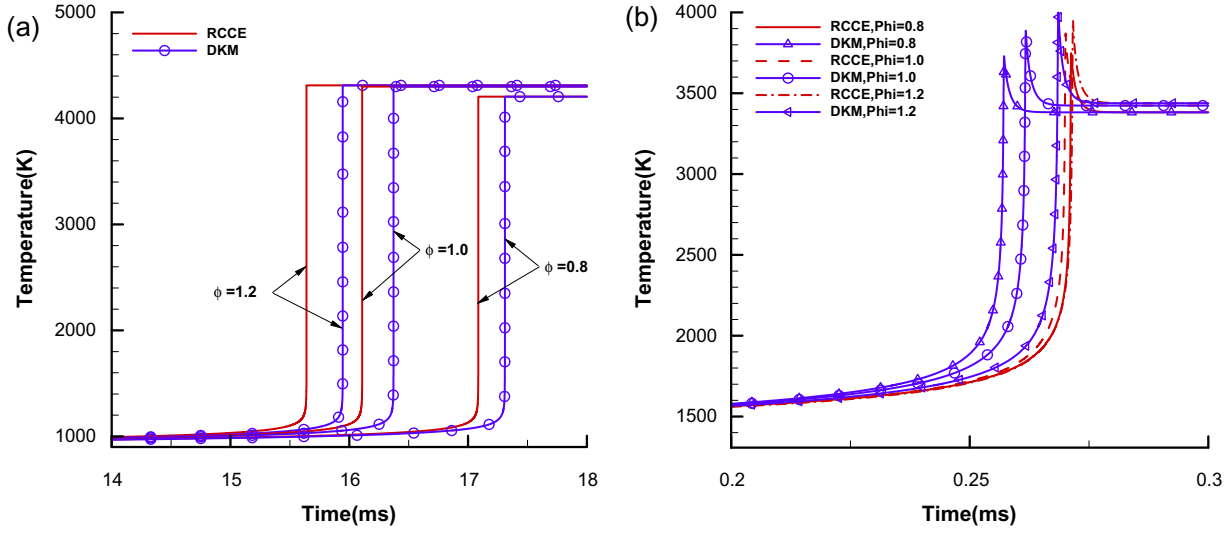

Fig. 3. Comparison of RCCE and DKM temperature vs. time profiles for CH_4/O_2 mixtures with different equivalence ratios at initial temperatures and pressures of 900 K and 100 atm (a) and 1500 K and 1 atm (b) (time in s).

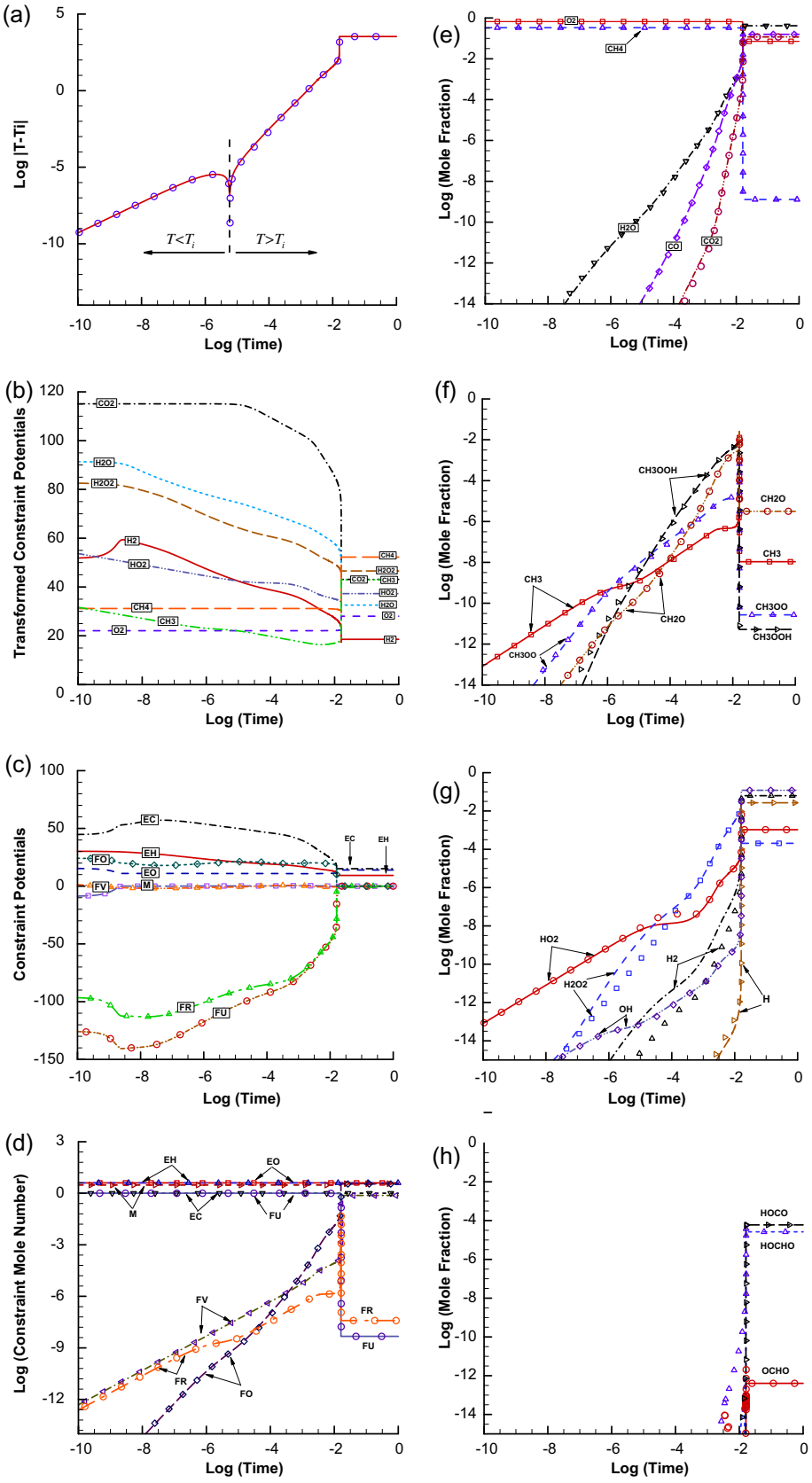

Fig. 4. Comparison of various RCCE and DKM time profiles for stoichiometric CH_4/O_2 mixtures at initial temperature and pressure of 900 K and 100 atm (time in s).

($\phi = 0.8$) mixtures and are shown in Fig. 3. RCCE predictions of ignition-delay-times at low temperature, high pressure are within 1% of those by DKM. At high temperature, low pressure the results agree within 1–5% of accuracy.

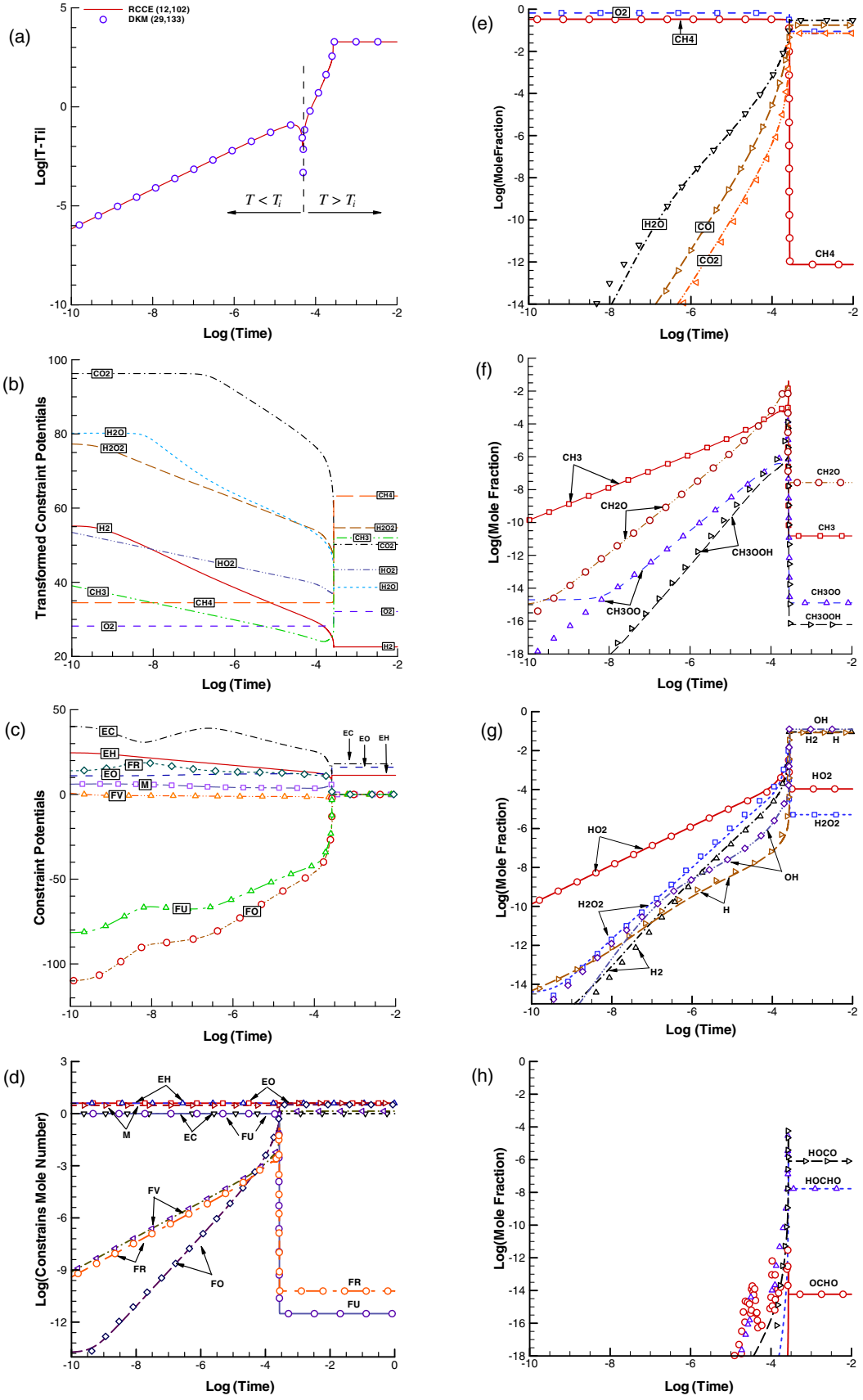

Fig. 5. Comparison of various RCCE and DKM time profiles for stoichiometric CH_4/O_2 mixtures at initial temperature and pressure of 1500 K and 1 atm (time in s).

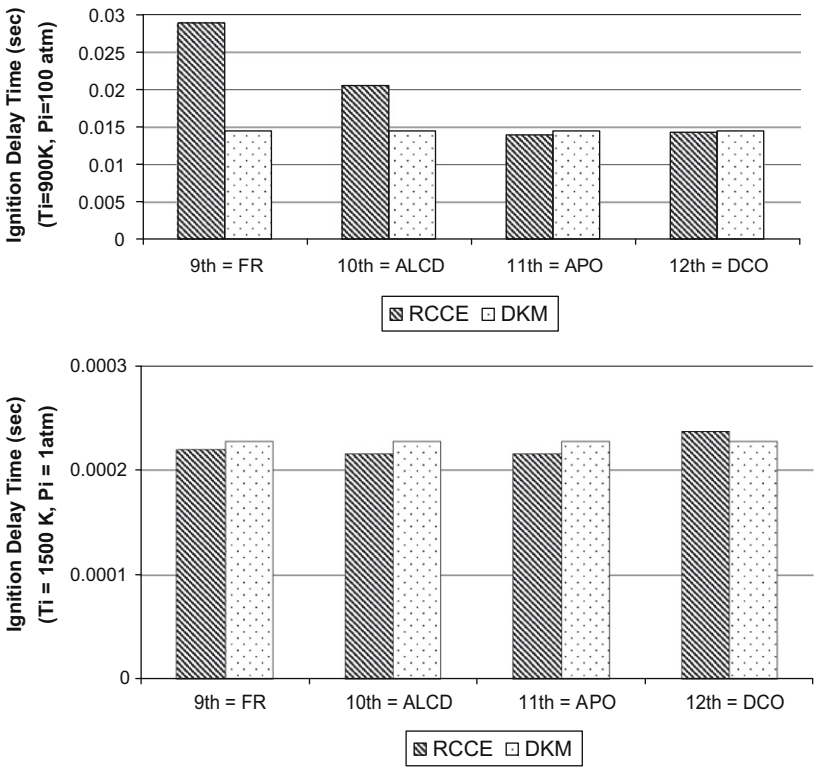

Fig. 6. Comparison of ignition-delay-times for RCCE models using 9–12 constraints with the DKM for stoichiometric CH_4/O_2 mixtures at initial temperatures and pressures of 900 K and 100 atm (top) and 1500 K and 1 atm (bottom).

Additional results are shown on log–log plots in Fig. 4 for the initial conditions 900 K and 100 atm, where the dominant radicals are $HO_2 \approx CH_3$ at early times and CH_3OO at late times, and in Fig. 5 for the initial conditions 1500 K and 1 atm, where the dominant radicals are $HO_2 \approx CH_3OO$ at all times. As can be seen in Figs. 3a and 4a, the temperature first decreases due to the fact that the

Table 3
Reduced reaction matrix $\underline{\underline{B}}$ for C_1 hydrocarbons (Units: cc, mole, kcal, s).

								X	X	X	X	X	X			CH_2O	Er	Uncert. factor
						X			X	X	X	X	X	X		CH_3OH		
					X	X			X	X	X	X	X	X	X	CH_4		
CH_2O	CH_3OH	CH_4	REK		CH_4	CH_3	CH_3OH	CH_2O	M	FV	FO	OHO	DCO	ALCD	APO	Log(Ar)		
		X	1	$CH_4 + O_2 = CH_3 + HO_2$	−1	1	0	0	0	2	0	0	0	0	0	13.6	57.3	5
		X	2	$CH_4 + HO_2 = CH_3 + H_2O_2$	−1	1	0	0	0	0	0	0	0	0	0	11.3	18.7	5
		X	3	$CH_4 + OH = CH_3 + H_2O$	−1	1	0	0	0	0	0	−1	0	0	0	13.5	2.1	1.4
		X	4	$CH_4 + CH_3OO = CH_3 + CH_3OOH$	−1	1	0	0	0	0	0	0	0	0	0	11.3	18.6	10
		X	5	$CH_3 + O_2 + M = CH_3OO + M$	0	−1	0	0	−1	0	0	0	0	0	1	12.0	0.0	3
		X	6	$CH_3 + O_2 = CH_3O + O$	0	−1	0	0	0	2	2	1	0	1	0	12.9	29.4	3
		X	7	$CH_3 + HO_2 = CH_3O + OH$	0	−1	0	0	0	0	2	1	0	1	0	13.3	0.0	3
		X	8	$CH_3 + CH_3OO = CH_3O + CH_3O$	0	−1	0	0	0	0	2	0	0	2	−1	13.4	0.0	3
	X		9	$CH_3OH + O_2 = CH_2OH + HO_2$	0	0	−1	0	0	2	0	0	0	0	0	13.4	45.2	10
	X		10	$CH_3OH + O_2 = CH_3O + HO_2$	0	0	−1	0	0	2	0	0	0	0	0	13.4	45.2	10
	X		11	$CH_3OH + HO_2 = CH_2OH + H_2O_2$	0	0	−1	0	0	0	0	0	0	0	0	11.0	12.6	10
	X		12	$CH_3OH + OH = CH_3O + H_2O$	0	0	−1	0	0	0	0	−1	0	0	0	13.7	1.5	2
X	X	X	13	$CH_2O + O_2 = CHO + HO_2$	0	0	0	−1	0	2	0	0	1	−1	0	14.0	40.0	2
X	X	X	14	$CH_2O + HO_2 = CHO + H_2O_2$	0	0	0	−1	0	0	0	0	1	−1	0	13.6	12.0	3
X	X	X	15	$CH_2O + OH = CHO + H_2O$	0	0	0	−1	0	0	0	−1	1	−1	0	13.7	−0.4	2
X	X	X	16	$H + O_2 + M = HO_2 + M$	0	0	0	0	−1	0	0	0	0	0	0	15.4	0.0	
X	X	X	17	$OH + H + M = H_2O + M$	0	0	0	0	−1	−2	0	−1	0	0	0	15.5	0.0	2
X	X	X	18	$OH + OH + M = H_2O_2 + M$	0	0	0	0	−1	−2	−2	−2	0	0	0	12.5	0.0	2
X	X	X	19	$H + O_2 = OH + O$	0	0	0	0	0	2	2	2	0	0	0	14.0	17.0	1.5
X	X	X	20	$CH_3OO + HO_2 = CH_3OOH + O_2$	0	0	0	0	0	−2	0	0	0	0	0	13.5	4.9	[5]
X	X	X	21	$HO_2 + HO_2 = H_2O_2 + O_2$	0	0	0	0	0	−2	0	0	0	0	0	11.1	−1.6	3
X	X	X	22	$CO + HO_2 = CO_2 + OH$	0	0	0	0	0	0	2	1	−1	0	0	14.2	23.6	3
X	X	X	23	$H + HO_2 = OH + OH$	0	0	0	0	0	0	2	2	0	0	0	14.1	0.9	2
X	X	X	24	$CO + OH = CO_2 + H$	0	0	0	0	0	0	0	−1	−1	0	0	11.8	0.1	1.5
12	16	20																

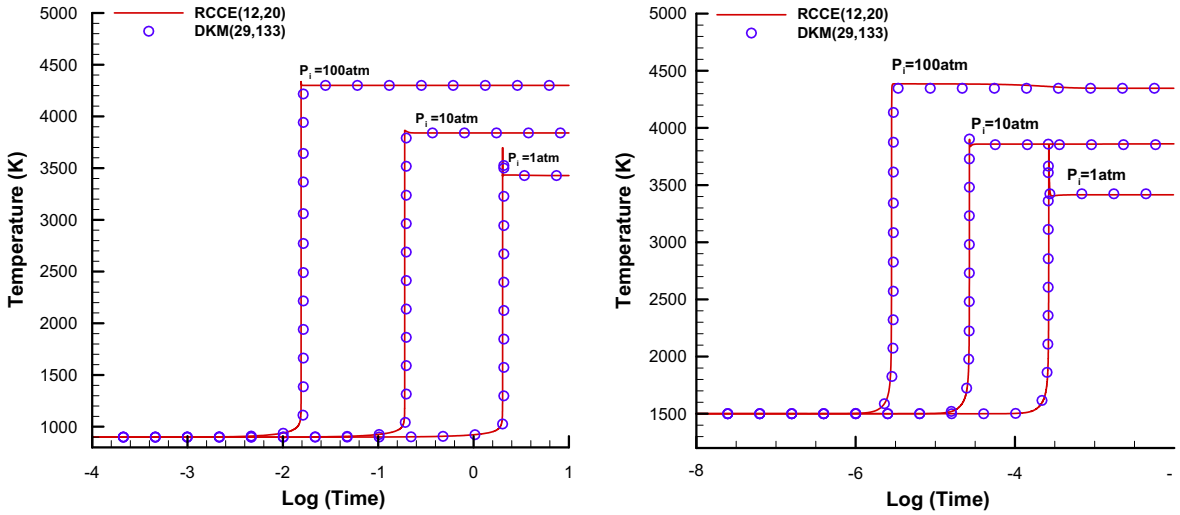

Fig. 7. Comparison of reduced RCCE(12, 20) and DKM temperature vs. time profiles for stoichiometric mixtures of CH_4/O_2 for different initial pressures at initial temperatures of 900 K (left) and 1500 K (right). The reduced RCCE(12, 20) model employed 12 constraints and 20 reactions listed in Table 3 (time in s).

initiation reactions are all endothermic then later increases as exothermic reactions become important. The agreement between RCCE and DKM calculations, especially with regard to the time at which the temperature difference becomes positive, is excellent.

Figs. 3b and 4b show the time dependence of the constraint potentials for the diagonalized constraint matrix and Figs. 3c and 4c show the corresponding constraint potentials for the primary constraint matrix. Note that for the primary constraint matrix, all the time-dependent constraint potentials go to zero at equilibrium as required, while those for the elements go to values identical with those obtained from the STANJAN equilibrium code [23]. Once the constraint potentials have been determined, the constrained-equilibrium mole fractions of any species for which the standard Gibbs free energy is known can be calculated from Eq. (3).

The fixed elemental constraints and the most important time-dependent constraints M, FV, FO, FU, and FR are shown in Figs. 3d and 4d and the mole fractions of the major species are shown in Figs. 3e–h and 4e–h. It can be seen that overall agreement is very good.

To investigate the sensitivity of the ignition-delay-time to the number of constraints used, a series of RCCE calculations was carried out starting with the eight constraints EH, EC, EO, M, FV, FO, OHO, and FU and adding additional constraints one at a time. The results for both high and low temperature conditions are compared with those of the DKM in Fig. 6. It can be seen that for high temperature conditions, nine constraints are sufficient to give the agreement within 5%, while for low temperature conditions, 11 constraints are required to give the same agreement.

5.1.2. Reduced CH_4 reaction mechanism

In the initial studies, a set of 133 reactions was used for both the RCCE and DKM calculations. As previously discussed, not all of these are of equal importance, especially in RCCE calculations where, in principle, only one independent reaction for each time-dependent constraint is required to allow the system to relax from the specified initial state to the correct final chemical-equilibrium state.

By systematically eliminating reactions, a reduced mechanism for C_1 hydrocarbons involving the 24 constraint-changing reactions in Table 3 has been found. The set of reactions used for the individual fuels: CH_4, CH_3OH and CH_2O, are indicated by cross marks in the left columns of the Table. The constraints

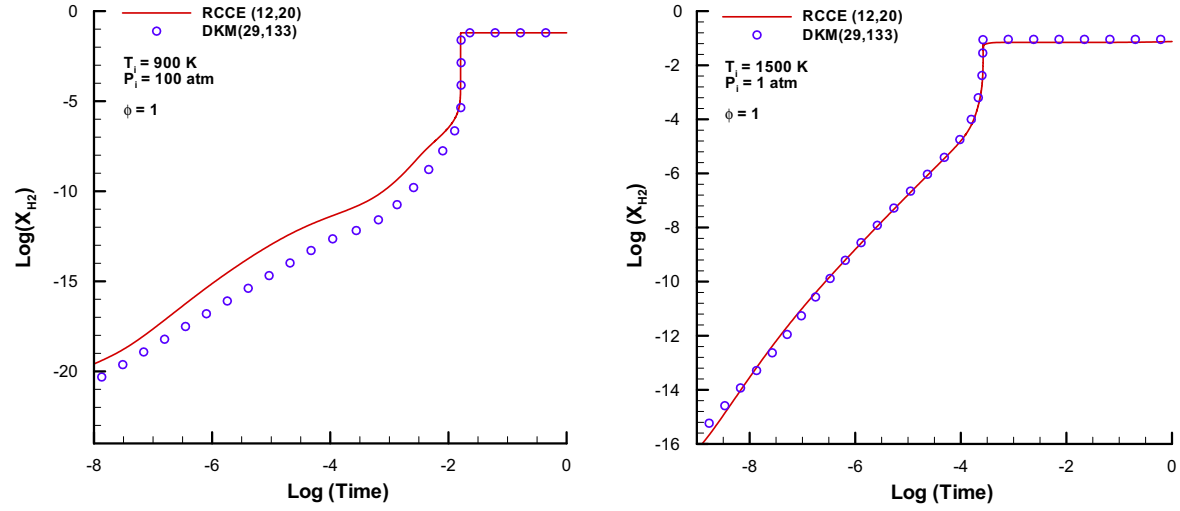

Fig. 8. Comparison of reduced RCCE(12, 20) and DKM H_2 mole fractions vs. time profiles for stoichiometric mixtures of CH_4/O_2 for different initial pressures at initial temperatures of 900 K (left) and 1500 K (right). Note that H_2 is not explicitly included in the RCCE (12, 20) model and the H_2 mole fractions were calculated from the constraint potentials.

used for each of the fuels are indicated by cross marks in the top rows of the Table. Arrhenius rate-parameters and uncertainty factors taken from Tsang and Hampson [22] are also shown in the right hand columns of the Table. It can be seen that many of the rates have estimate uncertainties greater than a factor of three even though these are among the simplest and best known reactions. For each constraint where more than one reaction is listed, the redundant reactions are important at different stages in the evolution of the system.

Reduced RCCE calculations for CH_4 were carried out using 12 constraints and 20 reactions. The temperature vs. time plots are shown in Fig. 7 and it can be seen that the RCCE calculations give ignition-delay-times within a few percent of those obtained using the DKM in both low and high temperature regimes.

In the RCCE approach, the moles of any species can be found from the constraint potentials using Eq. (3). It follows that any species which can be made from the elements will evolve dynamically even if there is no kinetic path provided in the mechanism. This

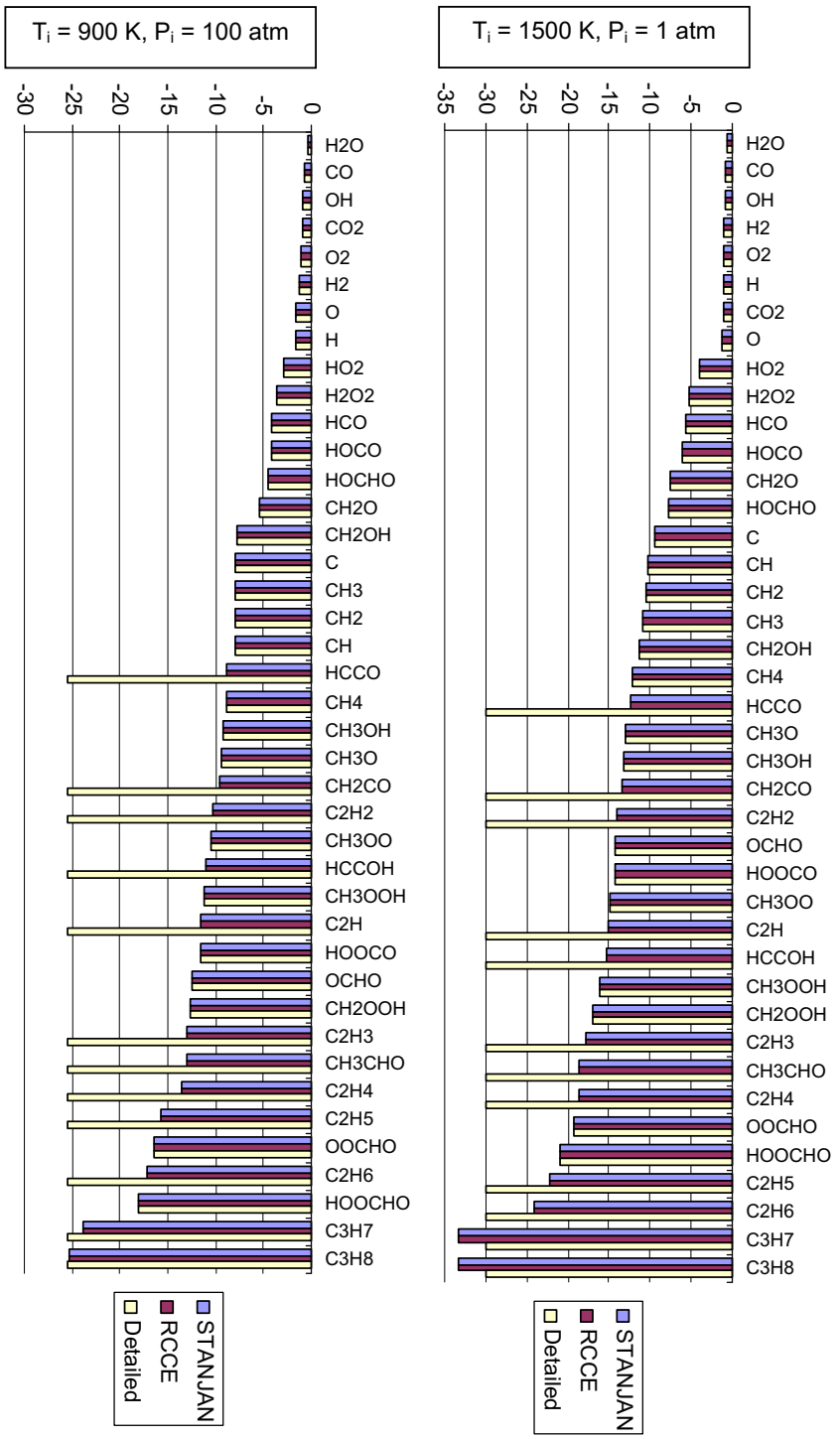

Fig. 9. Comparison of final C_1 and C_2 species mole fractions calculated using RCCE(12, 133) and DKM and C_1 kinetics with equilibrium mole fractions obtained using STANJAN for initial temperatures and pressures 900 K and 100 atm (left) and 1500 K and 1 atm (right). Note that the DKM C_2 mole fractions are frozen at the initial assigned values.

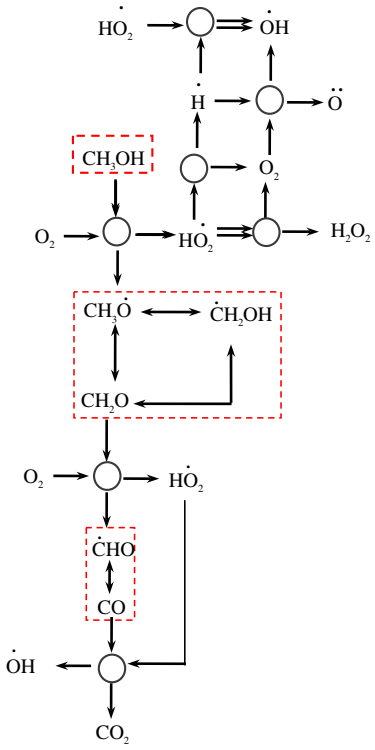

Fig. 10. RCCE reaction flow diagram of CH_3OH/O_2 oxidation.

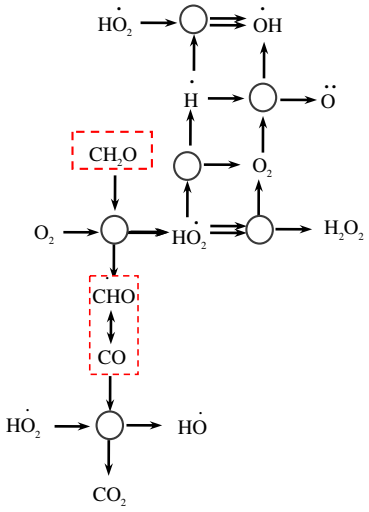

Fig. 12. RCCE reaction flow diagram for CH_2O/O_2 oxidation.

point is illustrated in Fig. 8 which compares reduced RCCE(12, 20) and DKM(29, 133) results for the mole fractions of H_2 as a function of time. Although no reactions involving H_2 are explicitly included in the RCCE(12, 20) calculations and H_2 is not on the species list, both the ignition-delay-time and the equilibrium mole fractions are in good agreement with the DKM(29, 133) results. This point is further illustrated in Fig. 9 where the final equilibrium mole fractions of the most abundant C_1 and C_2 species calculated using only C_1 kinetics in both the RCCE model and DKM are compared with values obtained using the STANJAN equilibrium code. For C_1 species, all values agree perfectly. However for C_2 species, the RCCE and STANJAN values agree but the DKM values are zero for the obvious reason that the list of species in the DKM does not include C_2 species. The ability to estimate the mole fractions of species not on a reaction list can be useful in determining whether they are likely to be kinetically important and therefore to be added to the model.

The fact that RCCE calculations can be carried out with fewer rate-equations than unknowns and still give constrained-equilibrium mole fractions for all species that can be made from the elements in the system is an important feature of the RCCE method that distinguishes it from most other reduction techniques that do not use a constrained-equilibrium manifold for reconstructing the missing species concentrations.

5.2. Methanol (CH_3OH) oxidation

The same set of basic constraints used for CH_4 can be used for the oxidation of methanol. However in this case, the fuel molecule FU is CH_3OH and fuel radical constraint, FR, is $CH_3O + CH_2OH + -CH_2O$. In addition, an examination of the kinetics shows that alkylperoxides reactions are not important and the APO constraint can be eliminated. This results in a reduction of the total number of

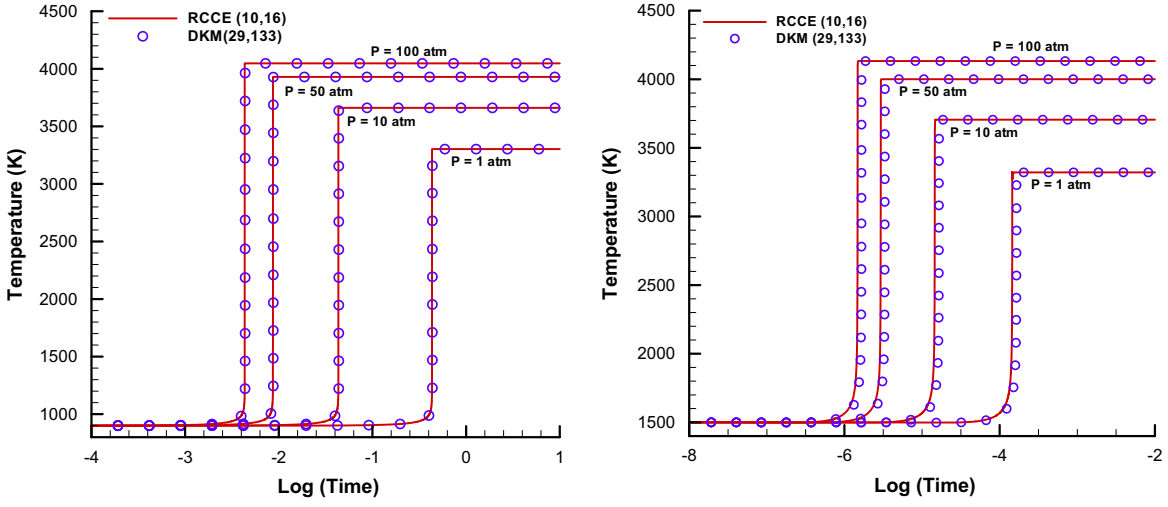

Fig. 11. Comparison of reduced RCCE(10, 16) and DKM temperature vs. time profiles for stoichiometric mixtures of CH_3OHOHO/O_2 for different initial pressures at initial temperatures of 900 K (left) and 1500 K (right). The reduced RCCE(10, 16) model for CH_3OHOHO/O_2 is shown in Table 3 (time in s).

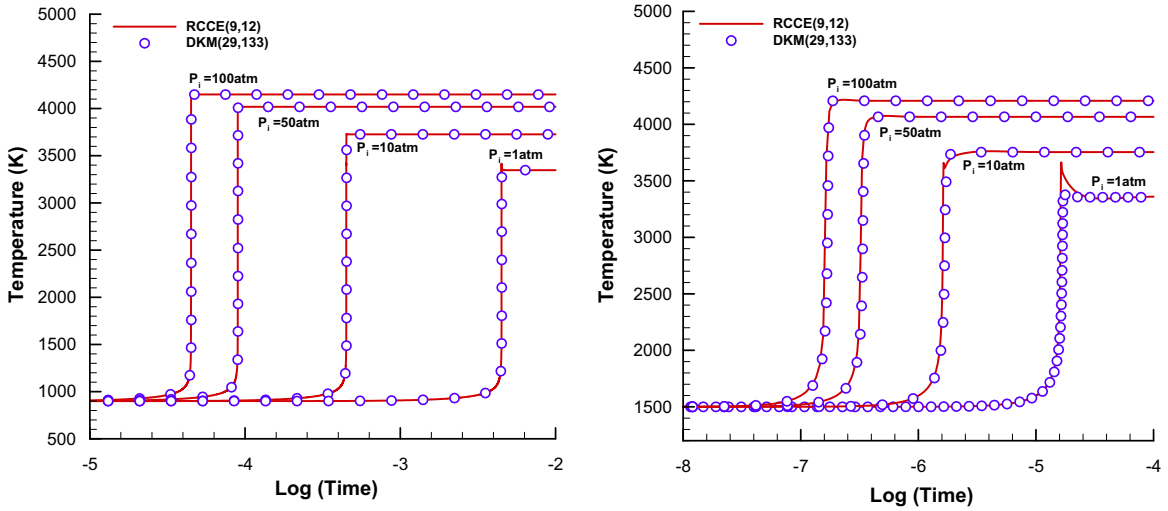

Fig. 13. Comparison of reduced RCCE(9, 12) and DKM temperature vs. time profiles for stoichiometric mixtures of CH_2OOHO/O_2 for different initial pressures at initial temperatures of 900 K (left) and 1500 K (right). The reduced RCCE(9, 12) model for CH_2OOHO/O_2 is shown in Table 3 (time in s).

constraints from 12 to 10. The corresponding reaction diagram is shown in Fig. 10.

5.2.1. Reduced CH_3OH reaction mechanism

A reduced set of 16 reactions for CH_3OH oxidation is included in Table 3. RCCE calculations using these reactions and the seven time-dependent constraints included in Table 3 are compared with DKM calculations using 133 reactions and 29 species in Fig. 11. It can be seen that the temperature vs. time plots are in excellent agreement over the entire range of temperature and pressure covered. The agreement for all other variables is similar to that for CH_4.

5.3. Formaldehyde (CH_2O) oxidation

The reaction diagram for CH_2O oxidation is shown in Fig. 12 and a reduced kinetic model is included in Table 3. The reduced kinetic model in this case is even simpler than that for CH_3OH and only nine constraints and 12 reactions are required in the RCCE calculations. A comparison of temperature vs. time plots is shown in Fig. 13 and again it can be seen that the agreement between RCCE and DKM calculations is excellent. As in the case of CH_3OH, plots of all other variables are also in excellent agreement and are similar to those for CH_4.

6. Summary and conclusions

RCCE calculations of methane, methanol and formaldehyde oxidation over a wide range of initial temperatures and pressures have been made using up to 12 constraints and 133 reactions and excellent agreement with "Detailed Kinetic Model" (DKM) calculations using 29 species and the same 133 reactions has been obtained. In addition, reduced sets of 20 reactions for methane, 16 reactions for methanol and 12 reactions for formaldehyde have been found, which when used in RCCE calculations give results identical to those obtained using the full 133 reactions.

Among the important features of the RCCE method for simplifying the kinetics of hydrocarbon oxidation are:

1. It is based on the well established Maximum Entropy Principle of Thermodynamics rather than mathematical approximations.
2. The entropy always increases as the system evolves and an approach to the final chemical-equilibrium state determined by the specified elements is guaranteed. This is not true for DKMs where only the listed species are included and all others are missing.
3. The total number of constraints required to determine the constrained-equilibrium state of a complex chemical system can be very much smaller than the number of species in the system, and an estimate of the concentrations of any species for which the standard Gibbs free energy is known can be obtained even though the species is not explicitly included in the model used.
4. Since the number of constraints required to determine the constrained-equilibrium state of a system can be very much smaller than the number of species in the system, fewer rate-equation are required to determine its evolution.
5. If the only constraints on the system are the elements and the state variables, RCCE calculations automatically reduce to local-thermodynamic-equilibrium (LTE) calculations.
6. If the number of constraints in an RCCE model is equal to the number of species in a DKM, the number of rate-equations will be the same but the species mole fractions will differ because the RCCE model will include all species which can be made from the elements but the DKM will include only the listed species.
7. The accuracy of the results can be improved by adding constraints one at a time until no further improvement is obtain. This can be done using either information available about probable rate-controlling reactions or trail and error.

Acknowledgments

This work was partially supported by ARO under technical monitoring of Dr. Ralph Anthenion. The authors are indebted to Dr. Yue Gao and Dr. Donald Goldthwaite for helpful comments and stimulating discussions.

References

[1] S.W. Benson, J. Chem. Phys. 20 (1952) 1605.
[2] M. Rein, Phys. Fluids A 4 (1992) 873.
[3] U. Mass, S.B. Pope, Combust. Flame 88 (1992) 239.
[4] S.H. Lam, D.A. Goussis, Proc. Combust. Inst. 22 (1988) 931.
[5] O. Oluwole, B. Bhattacharjee, J.E. Tolsma, P.I. Barton, W.H. Green, Combust. Flame 146 (1–2) (2006) 348–365.
[6] T. Lu, C.K. Law, Combust. Flame 144 (1–2) (2006) 24–36.
[7] Z. Ren, S.B. Pope, A. Vladimirsky, J.M.J. Guckenheimer, The ICE-PIC method for the dimension reduction of chemical kinetics, Chem. Phys. 124 (114111) (2006).
[8] J.C. Keck, D. Gillespie, Combust. Flame 17 (1971) 237.
[9] R. Law, M. Metghalchi, J.C. Keck, Proc. Combust. Inst. 22 (1988) 1705.

[10] P. Bishnu, D. Hamiroune, M. Metghalchi, J.C. Keck, Combust. Theory Model. 1 (1997) 295–312.
[11] D. Hamiroune, P. Bishnu, M. Metghalchi, J.C. Keck, Combust. Theory Model. 2 (1998) 81.
[12] V.A. Yousefian, Rate-controlled constrained-equilibrium thermochemistry algorithm for complex reacting systems, Combust. Flame 115 (1998) 66–80.
[13] Q. Tang, S.B. Pope, A more accurate projection in the rate-controlled constrained-equilibrium method for dimension reduction of combustion chemistry, Combust. Theory Model. (2004) 255–279.
[14] W.P. Jones, S. Rigopoulos, Rate-controlled constrained equilibrium: formulation and application of non-premixed laminar flames, Combust. Flame 142 (2005) 223–234.
[15] W.P. Jones, S. Rigopoulos, Reduced chemistry for hydrogen and methanol premixed flames via RCCE, Combust. Theory Model. 11 (5) (2007) 755–780.
[16] J.C. Keck, Prog. Energy Combust. Sci. 16 (1990) 125.
[17] P.S. Bishnu, D. Hamiroune, M. Metghalchi, Development of constrained equilibrium codes and their applications in nonequilibrium thermodynamics, J. Energy Resour. Technol. 123 (3) (2001) 2001.
[18] Y. Gao, Rate Controlled Constrained-Equilibrium Calculations of Formaldehyde Oxidation, Ph.D. Thesis, Northeastern University, Boston, 2003.
[19] S. Ugarte, Y. Gao, H. Metghalchi, Int. J. Therm. 3 (2005) 21.
[20] L. Petzold, SIAM J. Sci. Stat. Comput. 3 (1982) 367.
[21] <http://www.me.berkeley.edu/gri-mech/version30/text30.html>.
[22] W. Tsang, R.F. Hampson, J. Phys. Chem. Ref. Data 15 (3) (1986) 1087–1193.
[23] W.C. Reynolds, STANJAN Program, Stanford University, ME270, HO#7.